Application of the nonlinear Galerkin FEM method to the numerical solution of a reaction-diffusion system in two dimensions

By

Jan MACH[*]

Abstract

This paper deals with an application of the nonlinear Galerkin method to the numerical solution of a particular reaction-diffusion system in two spatial dimensions. This method was suggested as well adapted for the long-term integration of the evolution equations and combines the time and space discretization. Here we discuss the nonlinear Galerkin approach in the framework of the finite element method and give details on how the numerical scheme is derived. The modified Runge-Kutta method with adaptive time step selection is used for the integration in time. We also present the examples of numerical results.

§ 1.   Introduction

Consider the system of reaction-diffusion equations

$$(1.1) \qquad \frac{\partial U}{\partial t} = \mathbf{D}\Delta U + \mathbf{F}(U),$$

where $\mathbf{D} \in \mathbf{R}^{d,d}$ denotes a positively definite diagonal matrix, $\mathbf{F} : \mathbf{R}^d \to \mathbf{R}^d$ is a Lipschitz continuous mapping, $U(t, z)$ is a d-dimensional function of time $t \geq 0$ and of space $z \in \Omega \subset \mathbf{R}^n$. Ω is a bounded space domain with piecewise smooth boundary. We consider the homogeneous Neumann boundary conditions

$$(1.2) \qquad \frac{\partial U}{\partial \nu} = 0,$$

where ν is the unit outward normal of Ω and the initial condition

$$(1.3) \qquad\qquad U|_{t=0} = U_0 \in \mathbf{H},$$

where $\mathbf{H} := \mathbf{L}^2(\Omega, \mathbf{R}^d)$ is the Hilbert space with the scalar product

$$(1.4) \qquad (U, V) \equiv (U, V)_{\mathbf{H}} = \sum_{i=1}^{d} (U_i, V_i)_{\mathbf{H}} = \sum_{i=1}^{d} \int_{\Omega} U_i V_i,$$

and the space $\mathbf{V} := \mathbf{H}^{(1)}(\Omega, \mathbf{R}^d)$ as the Hilbert space with the scalar product

$$(1.5) \qquad (U, V)_{\mathbf{V}} = \sum_{i=1}^{d} (U_i, V_i)_{\mathbf{H}^{(1)}(\Omega)} = \sum_{i=1}^{d} \int_{\Omega} \nabla U_i \cdot \nabla V_i,$$

where $U = (U_1, \ldots, U_d)$, $V = (V_1, \ldots, V_d)$. The weak solution of the problem (1.1)-(1.3) on the time interval $(0, T)$ is a mapping $U : (0, T) \to \mathbf{V}$ such that it satisfies the following problem in the sense of distributions

$$(1.6) \qquad \frac{\mathrm{d}}{\mathrm{d}t}(U, W) + (\mathbf{D}U, W)_{\mathbf{V}} = (\mathbf{F}(U), W) \quad \text{in } (0, T) \; \forall W \in \mathbf{V},$$

$$(1.7) \qquad\qquad U|_{t=0} = U_0.$$

This abstract setting covers the initial-boundary value problems for wide range of reaction-diffusion systems, see e.g. [24, 28, 22].

The Gray-Scott model is the particular example of the reaction-diffusion system exhibiting rich dynamics [25], [26], [27]. It describes the autocatalytic chemical reaction

$$(1.8) \qquad\qquad U + 2V \to 3V, \quad V \to P,$$

where U, V are reactants and P is the final product of the reaction. The chemical substance U is being continuously added into the reactor and the product P is being continuously removed from the reactor during the reaction.

The initial-boundary value problem for the Gray-Scott model, considered in Section 3 for numerical simulations, is the following system

$$(1.9) \qquad\qquad \frac{\partial u}{\partial t} = D_u \Delta u - uv^2 + F(1 - u),$$

$$(1.10) \qquad\qquad \frac{\partial v}{\partial t} = D_v \Delta v + uv^2 - (F + k)v,$$

in $\Omega \times (0, T)$ with the initial conditions

$$(1.11) \qquad\qquad u(\cdot, 0) = u_{ini},$$

$$(1.12) \qquad\qquad v(\cdot, 0) = v_{ini}$$

and the zero Neumann boundary conditions

(1.13) $$\frac{\partial u}{\partial \nu}\mid_{\partial\Omega} = 0,$$

(1.14) $$\frac{\partial v}{\partial \nu}\mid_{\partial\Omega} = 0.$$

The functions u, v are unknowns representing concentrations of the chemical substances U, V. The parameter F denotes the rate at which the chemical substance U is being added during the chemical reaction, $F + k$ is the rate of the $V \to P$ transformation and a, b are the diffusion constants characterizing the environment of the reactor. We denote the reaction terms in the system (1.9)-(1.10) by $F_1(u, v)$, $F_2(u, v)$ or F_1, F_2 only. The system (1.9)-(1.13) has been studied from the viewpoint of qualitative behavior, see e.g. [24, 25, 26, 27] and of mathematical properties [28]. Mathematical consequences of these results help in the use of the presented method.

The rest of the article is organized as follows. The finite element nonlinear Galerkin scheme for the system of two reaction diffusion equations, i.e. the Gray-Scott model (1.9) - (1.10), is derived in Section 2. In Section 3 selected results of numerical solution are presented.

§ 2.   Nonlinear Galerkin method

The long-term behavior of dissipative systems to which (1.1) - (1.3) belongs can be described by the global attractor $\mathcal{A}$. In the standard Galerkin method the numerical solution of the problem under consideration is searched in the space $P_m\mathbf{H}$ spanned by $w_1, \ldots, w_n$ and thus produces an approximation of $\mathcal{A}$ in the space $P_m\mathbf{H}$. The nonlinear Galerkin method searches for the solution in an approximate inertial manifold, which is the nonlinear manifold closer to $\mathcal{A}$ than $P_m\mathbf{H}$ [1, 2, 3, 4]. This is the distinguishing property and the theoretical advantage of the nonlinear Galerkin approach compared to other simple methods. It was thus suggested as well adapted for the long-term integration of evolution equations in dynamically nontrivial situations [2]. It is general and allows the use of various methods for the time and space discretization of the underlaying problem. This approach was developed initially in the context of spectral methods [1, 2, 22]. Later, it has been generalized to other spatial discretization methods, i.e. the finite element method [7, 5, 14, 15, 23] and the finite difference method [12, 21].

The nonlinear Galerkin methods have been studied extensively. They have been applied to a variety of problems so far, i.e. to the modeling of turbulence [8, 10, 18], numerical solution of Navier-Stokes equations [5, 6, 11, 13, 23], the Kuramoto-Sivashinski equation [4, 16, 20] and the Burgers equation [9, 19, 20].

It has been also applied for the numerical simulations of reaction-diffusion systems, i.e. in [21] nonlinear Galerkin method based on the finite difference method is reported

to produce quantitatively the same results as the standard finite difference method when solving a particular reaction-diffusion system in two dimensions for parameters leading to non-trivial spatial and temporal behavior. In [22] the application of the non-linear Galerkin approach with the spectral spatial discretization to the one-dimensional Brusselator model is studied and it is reported to provide computational time savings compared to the standard Galerkin method with similar error in the numerical solution.

Reduction of the computational time for the same level of error was frequently reported as a computational advantage of the nonlinear Galerkin methods over the standard methods in other studies as well, see e.g. [4, 10, 11, 23]. Reported computational time gains varies between $25\% - 55\%$ depending on the particular nonlinear Galerkin scheme definition, implementation details and the studied problem. Some authors were not able to reproduce these positive results when using more sophisticated time integration methods with the adaptive time stepping [16, 20]. For comparison of different time integration methods in the context of nonlinear Galerkin methods see [17], where the author concludes that efficient integration in time is needed to avoid premature conclusion about the computational advantages of nonlinear Galerkin methods and to allow reliable comparison with the standard methods. Variable step-size variable formula BDF method was suggested as an efficient method for the time integration of those compared.

In our work we study whether the theoretical advantages can be converted into the computational ones for a particular nonlinear Galerkin method based on the finite element discretization in space. The finite element nonlinear Galerkin method is applied to the numerical integration of the system of two reaction-diffusion equations in two spatial dimensions. We provide details on how the the numerical scheme for the example problem is derived.

For $L > 0$ we denote

$$(2.1) \qquad\qquad\qquad \Omega \equiv (0, L) \times (0, L)$$

the square domain and remind here the notation $\mathbf{H} = \mathbf{L}^2(\Omega, \mathbf{R}^2)$ and $\mathbf{V} = \mathbf{H}^{(1)}(\Omega, \mathbf{R}^2)$. We consider the finite dimensional subspace $\mathbf{V}_h$ of $\mathbf{V}$ as in the usual Galerkin finite element method. In the nonlinear Galerkin method discussed here, $\mathbf{V}_h$ is decomposed into the coarse (large eddy) space $\mathbf{V}_{2h}$, and the correction space $\mathbf{W}_h$, as described in Section 2.1. That is $\mathbf{V}_h = \mathbf{V}_{2h} + \mathbf{W}_h$. The weak solution of the problem (1.6)-(1.7) is approximated by

$$(2.2) \qquad\qquad\qquad U_h(t) = Y_h(t) + Z_h(t),$$

where $\forall t > 0$, $Y_h(t) \in \mathbf{V}_{2h}$ and $Z_h(t) \in \mathbf{W}_h$. The function $Y_h(t)$ and $Z_h(t)$ are solutions

of the following equations, see i.e. [2, 22],

$$(2.3) \quad \frac{\mathrm{d}}{\mathrm{d}t}(Y_h, \tilde{Y}_h) + (\mathbf{D}Y_h + \mathbf{D}Z_h, \tilde{Y}_h)_{\mathbf{V}} = (\mathbf{F}(Y_h + Z_h), \tilde{Y}_h), \qquad \forall \tilde{Y}_h \in \mathbf{V}_{2h},$$

$$(2.4) \qquad (\mathbf{D}Y_h + \mathbf{D}Z_h, \tilde{Z}_h)_{\mathbf{V}} = (\mathbf{F}(Y_h) + \mathbf{F}'(Y_h) \cdot Z_h, \tilde{Z}_h), \quad \forall \tilde{Z}_h \in \mathbf{W}_h,$$

$$(2.5) \qquad (U|_{t=0}, \tilde{Y}_h) = (U_0, \tilde{Y}_h), \qquad \forall \tilde{Y}_h \in \mathbf{V}_{2h}.$$

The values of $Z_h(t)$ are known to be small for h small. At each time t, $U_h(t) \simeq Y_h(t)$, but the effect of the $Y_h(t)$ add up due to the sensitivity of reaction diffusion equation on the initial data and is thus effective on large intervals of time. The definition of functions $Y_h(t)$ and $Z_h(t)$ other than (2.3)-(2.5) is possible [16, 20].

The choice of the spaces $\mathbf{V}_{2h}$, $\mathbf{W}_h$ is given by the particular method of the space discretization - the finite element method in the case of this article, or the spectral method or the finite difference method, see [1, 2, 12, 21].

The framework of the convergence analysis for the nonlinear Galerkin method is given in [2, 3], and is elaborated for the reaction-diffusion systems in [22], and the finite-element method applied to them in [33].
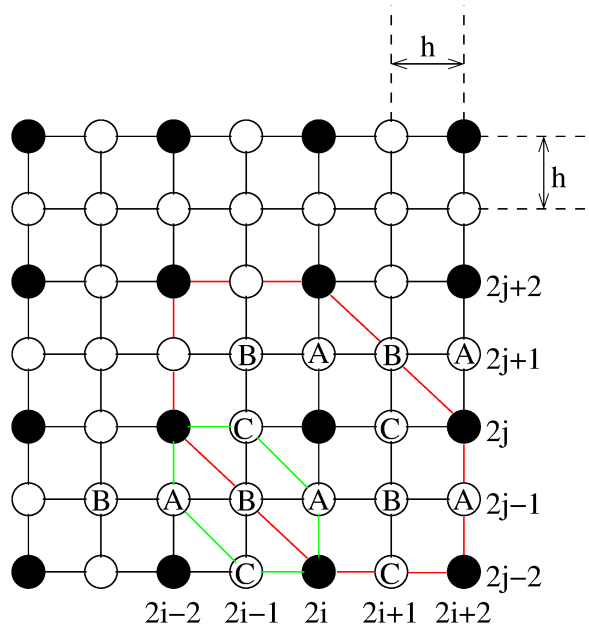

Figure 1. Numerical grid for the realization of the finite element nonlinear Galerkin method in two spatial dimensions.

§ 2.1. Discretization by the finite element method

In this section we describe details of the spatial discretization within the finite element nonlinear Galerkin method. For the square domain Ω (2.1), $N \in \mathcal{N}$, $h = L/2N$

we consider regular square mesh of nodes $x_{i,j} = [ih, jh]$, $i = 0, \ldots, 2N$, $j = 0, \ldots, 2N$, see Fig. 1. Let $\mathcal{E}_{2h}$ denote set of (black) node indices $[2i, 2j]$, $i = 0, \ldots, N$, $j = 0, \ldots, N$. In a similar manner we denote $\mathcal{E}_h$ the set of (white) node indices $[2i+1, 2j+1]$, $i = 0, \ldots, N-1$, $j = 0, \ldots, N-1$, $[2i, 2j+1]$, $i = 0, \ldots, N$, $j = 0, \ldots, N-1$ and $[2i+1, 2j]$, $i = 0, \ldots, N-1$, $j = 0, \ldots, N$.

The piecewise linear finite elements are used to construct the corresponding spaces. First, we define the nodal (hat) functions φ_O, $\forall O \in \mathcal{E}_{2h}$ that are equal to one at nodes x_O and are equal to zero at all other nodes x_M, $\forall M \in \mathcal{E}_{2h}$, $M \neq 0$.

Next, we define the nodal (hat) functions ψ_P, $\forall P \in \mathcal{E}_h$ that are equal to one at nodes x_P and are equal to zero at all other nodes x_M, $\forall M \in \mathcal{E}_h$, $M \neq P$.

We define

$$(2.6) \qquad \left[\varphi_{2i,2j}^{(1)} = \begin{pmatrix} \varphi_{2i,2j} \\ 0 \end{pmatrix}, \varphi_{2i,2j}^{(2)} = \begin{pmatrix} 0 \\ \varphi_{2i,2j} \end{pmatrix} \right]_{i=0,j=0}^{N,N},$$

$$(2.7) \qquad \left[\psi_{2i+1,2j}^{(1)} = \begin{pmatrix} \psi_{2i+1,2j} \\ 0 \end{pmatrix}, \psi_{2i+1,2j}^{(2)} = \begin{pmatrix} 0 \\ \psi_{2i+1,2j} \end{pmatrix} \right]_{i=0,j=0}^{N-1,N},$$

$$(2.8) \qquad \left[\psi_{2i,2j+1}^{(1)} = \begin{pmatrix} \psi_{2i,2j+1} \\ 0 \end{pmatrix}, \psi_{2i,2j+1}^{(2)} = \begin{pmatrix} 0 \\ \psi_{2i,2j+1} \end{pmatrix} \right]_{i=0,j=0}^{N,N-1},$$

$$(2.9) \qquad \left[\psi_{2i+1,2j+1}^{(1)} = \begin{pmatrix} \psi_{2i+1,2j+1} \\ 0 \end{pmatrix}, \psi_{2i+1,2j+1}^{(2)} = \begin{pmatrix} 0 \\ \psi_{2i+1,2j+1} \end{pmatrix} \right]_{i=0,j=0}^{N-1,N-1},$$

as the 2-dimensional vector-valued finite element basis functions. The basis of $\mathbf{V}_{2h}$ consists of functions (2.6). The space $\mathbf{W}_h$ is spanned by functions (2.7), (2.8) and (2.9). The union of the bases of $\mathbf{V}_{2h}$ and $\mathbf{W}_h$ provides a hierarchical (induced) basis of $\mathbf{V}_h$.

Specifying $Y_h = (u_h, v_h)$ and $Z_h = (z_h, w_h)$ in the numerical approximation (2.2) we have

$$(2.10) \qquad u_{2h} = \sum_{i=0,j=0}^{N,N} u_{2i,2j} \varphi_{2i,2j},$$

$$(2.11) \qquad v_{2h} = \sum_{i=0,j=0}^{N,N} v_{2i,2j} \varphi_{2i,2j},$$

$$(2.12) \qquad z_h = \sum_{i=0,j=0}^{N-1,N} z_{2i+1,2j} \psi_{2i+1,2j} + \sum_{i=0,j=0}^{N,N-1} z_{2i,2j+1} \psi_{2i,2j+1}$$

$$+ \sum_{i=0,j=0}^{N-1,N-1} z_{2i+1,2j+1}\psi_{2i+1,2j+1},$$

$$(2.13) \qquad w_h = \sum_{i=0,j=0}^{N-1,N} w_{2i+1,2j}\psi_{2i+1,2j} + \sum_{i=0,j=0}^{N,N-1} w_{2i,2j+1}\psi_{2i,2j+1}$$

$$+ \sum_{i=0,j=0}^{N-1,N-1} w_{2i+1,2j+1}\psi_{2i+1,2j+1}.$$

where the components of the principle solution part Y_h and of the correction term Z_h are the solution of the following system

$$(2.14) \qquad \partial_t(u_{2h},\varphi_O) + D_u(u_{2h} + z_h, \varphi_O)_V = (F_1(u_{2h} + z_h, v_{2h} + w_h), \varphi_O),$$

$$(2.15) \qquad \partial_t(v_{2h},\varphi_O) + D_v(v_{2h} + w_h, \varphi_O)_V = (F_2(u_{2h} + z_h, v_{2h} + w_h), \varphi_O),$$

$$(2.16) \qquad D_u(u_{2h} + z_h, \psi_P)_V = (F_1(u_{2h}, v_{2h}) + \partial_u F_1(u_{2h}, v_{2h})z_h$$
$$+ \partial_v F_1(u_{2h}, v_{2h})w_h, \psi_P),$$

$$(2.17) \qquad D_v(v_{2h} + w_h, \psi_P)_V = (F_2(u_{2h}, v_{2h}) + \partial_u F_2(u_{2h}, v_{2h})z_h$$
$$+ \partial_v F_2(u_{2h}, v_{2h})w_h, \psi_P).$$

$\forall O \in \mathcal{E}_{2h}$ and $\forall P \in \mathcal{E}_h$, which corresponds to (2.3) - (2.4) for $\mathbf{D} = diag\{D_u, D_v\}$ and $\mathbf{F} = (F_1, F_2)$. We denote here $(\cdot, \cdot)$ and $(\cdot, \cdot)_V$ scalar product (1.4) and bilinear form (1.5) for $d = 1$ respectively.

Now we derive equations for the term z_h from (2.16). Equations for w_h are derived analogously. Numerical integration is applied to approximate the right-hand side of (2.16). For the particular index $P \in \mathcal{E}_h$, such that $x_P \cap \partial\Omega = \emptyset$, the following approximation is used

$$(2.18) \qquad (F_1 + \partial_u F_1 + \partial_v F_1, \psi_P) \sim h^2 F_1|_P + h^2 \partial_u F_1|_P + h^2 \partial_v F_1|_P,$$

which can be modified for the boundary nodes replacing h^2 terms by $\frac{1}{2}h^2$.

We consider ψ_P, $P \in \mathcal{E}_h$ defined at nodes $x_{2i,2j+1}$, $x_{2i+1,2j+1}$ and $x_{2i+1,2j}$ separately. For $\psi_P \equiv \psi_{2i,2j+1}$, $0 \le j < N$ in (2.16) we receive

$$(2.19) \qquad (u_{2h} + z_h, \psi_{2i,2j+1})_V = (u_{2h}, \psi_{2i,2j+1})_V + (z_h, \psi_{2i,2j+1})_V$$
$$= \frac{1}{2}(u_{2i,2j} + u_{2i,2j+2} - u_{2i-2,2j+2} - u_{2i+2,2j})$$
$$- z_{2i-1,2j+1} + 4z_{2i,2j+1} - z_{2i+1,2j+1},$$

for $0 < i < N$. For $i = 0$ and $i = N$ we have

$$(2.20) \qquad (u_{2h} + z_h, \psi_{0,2j+1})_V = (u_{2h}, \psi_{0,2j+1})_V + (z_h, \psi_{0,2j+1})_V$$

$$= \frac{1}{2}(u_{0,2j} - u_{2,2j}) + 2z_{0,2j+1} - z_{1,2j+1},$$

and

$$(2.21) \qquad (u_{2h} + z_h, \psi_{2N,2j+1})_V = (u_{2h}, \psi_{2N,2j+1})_V + (z_h, \psi_{2N,2j+1})_V$$
$$= \frac{1}{2}u_{2N,2j+2} - z_{2N-1,2j+1} + 2D_u z_{2N,2j+1},$$

respectively. Finally, for $0 < i < N$, the equation (2.16) yields

$$(2.22) \qquad -\frac{D_u}{h^2}z_{2i-1,2j+1} + \left(\frac{4D_u}{h^2} - \partial_u F_1|_{2i,2j+1}\right)z_{2i,2j+1}$$

$$-\frac{D_u}{h^2}z_{2i+1,2j+1} - \partial_v F_1|_{2i,2j+1}w_{2i,2j+1}$$

$$= F_1|_{2i,2j+1} - \frac{D_u}{2h^2}(u_{2i,2j} + u_{2i,2j+2} - u_{2i-2,2j+2} - u_{2i+2,2j}).$$

For $i = 0$ and $i = N$ we have

$$(2.23) \quad \left(\frac{4D_u}{h^2} - \partial_u F_1|_{0,2j+1}\right)z_{0,2j+1} - \frac{2D_u}{h^2}z_{1,2j+1} - \partial_v F_1|_{0,2j+1}w_{0,2j+1}$$

$$= F_1|_{0,2j+1} - \frac{D_u}{h^2}(u_{0,2j} - u_{2,2j}),$$

and

$$(2.24) -\frac{2D_u}{h^2}z_{2N-1,2j+1} + \left(\frac{4D_u}{h^2} - \partial_u F_1|_{2N,2j+1}\right)z_{2N,2j+1} - \partial_v|_{2N,2j+1}w_{2N,2j+1}$$

$$= F_1|_{2N,2j+1} - \frac{D_u}{h^2}(u_{2N,2j+2} - u_{2N-2,2j+2}),$$

respectively.

For $\psi_P \equiv \psi_{2i+1,2j+1}$, $0 \leq i < N$ and $0 \leq j < N$ in (2.16) we get

$$(2.25) \qquad (u_{2h} + z_h, \psi_{2i+1,2j+1})_V = (u_{2h}, \psi_{2i+1,2j+1})_V + (z_h, \psi_{2i+1,2j+1})_V$$
$$= (u_{2i,2j+2} + u_{2i+2,2j} - u_{2i,2j} - u_{2i+2,2j+2}) - z_{2i+1,2j}$$
$$-z_{2i,2j+1} + 4z_{2i+1,2j+1} - z_{2i+2,2j+1} - z_{2i+1,2j+2}$$

and thus equation (2.16) yields

$$(2.26) \qquad -\frac{D_u}{h^2}z_{2i+1,2j} - \frac{D_u}{h^2}z_{2i,2j+1} + \left(\frac{4D_u}{h^2} - \partial_u F_1|_{2i+1,2j+1}\right)z_{2i+1,2j+1}$$

$$-\frac{D_u}{h^2}z_{2i+2,2j+1} - \frac{D_u}{h^2}z_{2i+1,2j+2} - \partial_v F_1|_{2i+1,2j+1}w_{2i+1,2j+1}$$

$$= F_1|_{2i+1,2j+1} - \frac{D_u}{h^2}(u_{2i,2j+2} + u_{2i+2,2j} - u_{2i,2j} - u_{2i+2,2j+2}).$$

For $\psi_P \equiv \psi_{2i+1,2j}$, $0 \le i < N$ in (2.16) we get

$$
(2.27) \qquad (u_{2h} + z_h, \psi_{2i+1,2j})_V = (u_{2h}, \psi_{2i+1,2j})_V + (z_h, \psi_{2i+1,2j})_V
$$
$$
= \frac{1}{2}(-u_{2i+2,2j-2} + u_{2i+2,2j} + u_{2i,2j} - u_{2i,2j+2})
$$
$$
-z_{2i+1,2j-1} + 4z_{2i+1,2j} - z_{2i+1,2j+1},
$$

for $0 < j < N$. For $j = 0$ and $j = N$ we have

$$
(2.28) \qquad (u_{2h} + z_h, \psi_{2i+1,0})_V = (u_{2h}, \psi_{2i+1,0})_V + (z_h, \psi_{2i+1,0})_V
$$
$$
= \frac{1}{2}(u_{2i,0} - u_{2i,2}) + 2z_{2i+1,0} - z_{2i+1,1},
$$

and

$$
(2.29) \qquad (u_{2h} + z_h, \psi_{2i+1,2N})_V = (u_{2h}, \psi_{2i+1,2N})_V + (z_h, \psi_{2i+1,2N})_V
$$
$$
= \frac{1}{2}(u_{2i+2,2N} - u_{2i+2,2N-2}) - z_{2i+1,2N-1} + 2z_{2i+1,2N}
$$

respectively. Finally, the equation (2.16) yields

$$
(2.30) \qquad -\frac{D_u}{h^2}z_{2i+1,2j-1} + \left(\frac{4D_u}{h^2} - \partial_u F_1|_{2i+1,2j}\right)z_{2i+1,2j} - \frac{D_u}{h^2}z_{2i+1,2j+1}
$$
$$
-\partial_v F_1|_{2i+1,2j}w_{2i+1,2j}
$$
$$
= F_1|_{2i+1,2j} - \frac{D_u}{2h^2}(-u_{2i+2,2j-2} + u_{2i+2,2j} + u_{2i,2j} - u_{2i,2j+2}),
$$

for $0 < j < N$. For $j = 0$ and $j = N$ we obtain

$$
(2.31) \qquad \left(\frac{4D_u}{h^2} - \partial_u F_1|_{2i+1,0}\right)z_{2i+1,0} + -\frac{2D_u}{h^2}z_{2i+1,1} - \partial_v F_1|_{2i+1,0}w_{2i+1,0}
$$
$$
= F_1|_{2i+1,0} - \frac{D_u}{h^2}(u_{2i,0} - u_{2i,2}),
$$

and

$$
(2.32) \quad -\frac{2D_u}{h^2}z_{2i+1,2N-1} + \left(\frac{4D_u}{h^2} - \partial_u F_1|_{2i+1,2N}\right)z_{2i+1,2N} - \partial_v F_1|_{2i+1,2N}w_{2i+1,2N}
$$
$$
= F_1|_{2i+1,2N} - \frac{D_u}{h^2}(u_{2i+2,2N} - u_{2i+2,2N-2}),
$$

respectively.

We need to evaluate terms u_{2h}, v_{2h} at grid nodes x_P, $\forall P \in \mathcal{E}_h$ to compute values of $F_1|_P$, $\partial_u F_1|_P$ and $\partial_v F_1|_P$. This is accomplished by the linear interpolation

$$
(2.33) \qquad u_{2h}|_{2i+1,2j} = \frac{1}{2}(u_{2i,2j} + u_{2i+2,2j}),
$$

$$(2.34) \qquad u_{2h}|_{2i,2j+1} = \frac{1}{2}(u_{2i,2j} + u_{2i,2j+2}),$$

$$(2.35) \qquad u_{2h}|_{2i+1,2j+1} = \frac{1}{2}(u_{2i,2j+2} + u_{2i+2,2j}).$$

In the similar manner, the term v_{2h} is treated.

We obtained the sparse linear system of $2n_{corr}$,

$$n_{corr} = (N+1)N + N(2N+1) = N(3N+2),$$

equations for the values of terms z_h, w_h at grid nodes x_P, $P \in \mathcal{E}_h$. The matrix is stored in compressed sparse column (CSC) representation for use with the $UMFPACK$ solver [29, 30, 31, 32], which we use to solve the system.

Now we derive equations for the values of the solution component u_{2h} from (2.14). Equations for v_{2h} in (2.15) are derived analogously. Numerical integration is used to approximate the right-hand side (2.14) For particular $O \in \mathcal{E}_{2h}$, such that $x_O \cap \partial\Omega = \emptyset$, the following approximation is used

$$(2.36) \quad (F_1(u_{2h} + z_h, v_{2h} + w_h), \varphi_O) \sim \sum_{P \in \mathcal{E}_h} h^2 \varphi_O|_P F_1(u_{2h} + z_h, v_{2h} + w_h)|_P.$$

The term h^2 is the area around grid nodes x_P, $P \in \mathcal{E}_h$ as it is depicted in Fig. 2. For $\varphi_O \equiv \varphi_{2i,2j}$, $0 < i < N$, $0 < j < N$ and denoting $F_1 \equiv F_1(u_{2h} + z_h, v_{2h} + w_h)$ the approximation (2.36) yields

$$(2.37) \qquad (F_1, \varphi_{2i,2j}) \sim \frac{1}{2}h^2 F_1|_{2i,2j-1} + \frac{1}{2}h^2 F_1|_{2i+1,2j-1} + \frac{1}{2}h^2 F_1|_{2i-1,2j}$$

$$+ h^2 F_1|_{2i,2j} + \frac{1}{2}h^2 F_1|_{2i+1,2j} + \frac{1}{2}h^2 F_1|_{2i-1,2j+1} + \frac{1}{2}h^2 F_1|_{2i,2j+1},$$

which can be modified for the boundary nodes.

We need to evaluate the terms $u_{2h} + z_h$, $v_{2h} + w_h$ at grid nodes x_P, $\forall P \in \mathcal{E}_h$ in the approximation (2.36). Linear interpolation is used to interpolate values of u_{2h}, v_{2h} on grid nodes x_P, $\forall P \in \mathcal{E}_h$

$$(2.38) \qquad (u_{2h} + z_h)|_{2i+1,2j} = \frac{1}{2}(u_{2i,2j} + u_{2i+2,2j}) + z_{2i+1,2j},$$

$$(2.39) \qquad (u_{2h} + z_h)|_{2i,2j+1} = \frac{1}{2}(u_{2i,2j} + u_{2i,2j+2}) + z_{2i,2j+1},$$

$$(2.40) \qquad (u_{2h} + z_h)|_{2i+1,2j+1} = \frac{1}{2}(u_{2i,2j+2} + u_{2i+2,2j}) + z_{2i+1,2j+1}.$$

In the similar manner, the term $v_{2h} + w_h$ is treated.

For a particular nodal hat function $\varphi_O \equiv \varphi_{2i,2j}$, $0 < i < N$, $0 < j < N$ in Eq. (2.14) we derive

$$(2.41) \quad \frac{1}{3}h^2 \dot{u}_{2i,2j-2} + \frac{1}{3}h^2 \dot{u}_{2i+2,2j-2} + \frac{1}{3}h^2 \dot{u}_{2i-2,2j} + 2h^2 \dot{u}_{2i,2j}$$
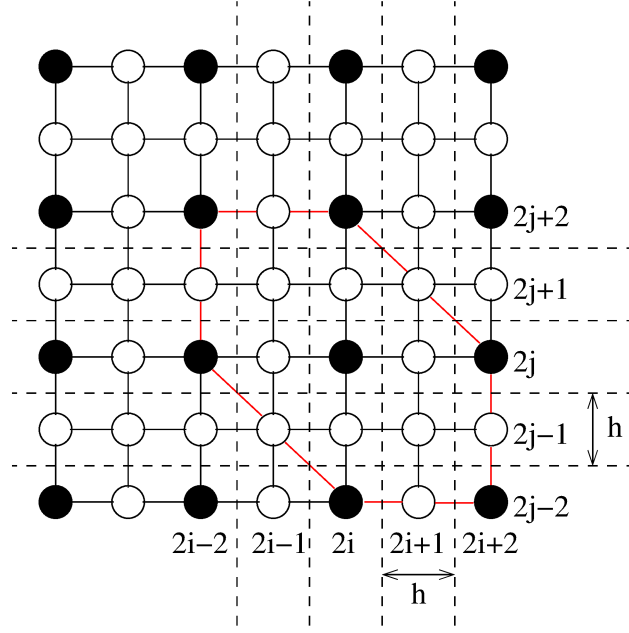
Figure 2. Numerical integration.

$$+\frac{1}{3}h^2\dot{u}_{2i+2,2j} + \frac{1}{3}h^2\dot{u}_{2i-2,2j+2} + \frac{1}{3}h^2\dot{u}_{2i,2j+2} - D_u u_{2i,2j-2}$$

$$-D_u u_{2i-2,2j} + 4D_u u_{2i,2j} - D_u u_{2i+2,2j} - D_u u_{2i,2j+2} - \frac{1}{2}D_u z_{2i+1,2j-2}$$

$$-D_u z_{2i-1,2j-1} + \frac{1}{2}D_u z_{2i,2j-1} + D_u z_{2i+1,2j-1} - \frac{1}{2}D_u z_{2i+2,2j-1}$$

$$+\frac{1}{2}D_u z_{2i-1,2j} + \frac{1}{2}D_u z_{2i+1,2j} - \frac{1}{2}D_u z_{2i-2,2j+1} + D_u z_{2i-1,2j+1}$$

$$+\frac{1}{2}D_u z_{2i,2j+1} - D_u z_{2i+1,2j+1} - \frac{1}{2}D_u z_{2i-1,2j+2}$$

$$=\frac{1}{2}h^2 F_1|_{2i,2j-1} + \frac{1}{2}h^2 F_1|_{2i+1,2j-1} + \frac{1}{2}h^2 F_1|_{2i-1,2j} + h^2 F_1|_{2i,2j}$$

$$+\frac{1}{2}h^2 F_1|_{2i+1,2j} + \frac{1}{2}h^2 F_1|_{2i-1,2j+1} + \frac{1}{2}h^2 F_1|_{2i,2j+1}.$$

For $\varphi_O \equiv \varphi_{0,0}$ we obtain

$$(2.42) \qquad \frac{1}{3}h^2\dot{u}_{0,0} + \frac{1}{6}h^2\dot{u}_{2,0} + \frac{1}{6}h^2\dot{u}_{0,2} + D_u u_{0,0} - \frac{1}{4}D_u u_{2,0}$$

$$-\frac{1}{2}D_u u_{0,2} + \frac{1}{2}D_u z_{1,0} + \frac{1}{2}D_u z_{0,1} - D_u z_{1,1}$$

$$=\frac{1}{4}h^2 F_1|_{0,0} + \frac{1}{4}h^2 F_1|_{1,0} + \frac{1}{4}h^2 F_1|_{0,1}.$$

For $\varphi_O \equiv \varphi_{2i,0}$, $0 < i < N$ the Eq. (2.14) gives

$$(2.43) \quad \frac{1}{6}h^2\dot{u}_{2i-2,0} + h^2\dot{u}_{2i,0} + \frac{1}{6}h^2\dot{u}_{2i+2,0} + \frac{1}{3}h^2\dot{u}_{2i-2,2} + \frac{1}{3}h^2\dot{u}_{2i,2}$$

$$-\frac{1}{2}D_u u_{2i-2,0} + 2D_u u_{2i,0} - \frac{1}{2}D_u u_{2i+2,0} - D_u u_{2i,2} + \frac{1}{2}D_u z_{2i+1,0}$$

$$-\frac{1}{2}D_u z_{2i-2,1} + D_u z_{2i-1,1} + \frac{1}{2}D_u z_{2i,1} - D_u z_{2i+1,1} - \frac{1}{2}D_u z_{2i-1,2}$$

$$= \frac{1}{4}h^2 F_1|_{2i-1,0} + \frac{1}{2}h^2 F_1|_{2i,0} + \frac{1}{4}h^2 F_1|_{2i+1,0} + \frac{1}{2}h^2 F_1|_{2i-1,1} + \frac{1}{2}h^2 F_1|_{2i,1}.$$

For $\varphi_O \equiv \varphi_{2N,0}$ the Eq. (2.14) yields

$$(2.44) \qquad \frac{1}{6}h^2 \dot{u}_{2N-2,0} + \frac{2}{3}h^2 \dot{u}_{2N,0} + \frac{1}{3}h^2 \dot{u}_{2N-2,2} + \frac{1}{6}h^2 \dot{u}_{2N,2}$$

$$-\frac{1}{2}D_u u_{2N-2,0} + D_u u_{2N,0} - \frac{1}{2}D_u u_{2N,2} - \frac{1}{2}D_u z_{2N-2,1}$$

$$+D_u z_{2N-1,1} - \frac{1}{2}D_u z_{2N-1,2}$$

$$= \frac{1}{4}h^2 F_1(|_{2N-1,0} + \frac{1}{4}h^2 F_1|_{2N,0} + \frac{1}{2}h^2 F_1|_{2N-1,1} + \frac{1}{4}h^2 F_1|_{2N,1}.$$

For $\varphi_O \equiv \varphi_{0,2j}$, $0 < j < N$ we have

$$(2.45)\ \frac{1}{6}h^2 \dot{u}_{0,2j-2} + \frac{1}{3}h^2 \dot{u}_{2,2j-2} + h^2 \dot{u}_{0,2j} + \frac{1}{3}h^2 \dot{u}_{2,2j}$$

$$+\frac{1}{6}h^2 \dot{u}_{0,2j+2} - \frac{1}{2}D_u u_{0,2j-2} + 2D_u u_{0,2j} - D_u u_{2i+2,2j}$$

$$-\frac{1}{2}D_u u_{0,2j+2} - \frac{1}{2}D_u z_{1,2j-2} + D_u z_{1,2j-1} - \frac{1}{2}D_u z_{2,2j-1}$$

$$+\frac{1}{2}D_u z_{1,2j} + \frac{1}{2}D_u z_{0,2j+1} - D_u z_{1,2j+1}$$

$$= \frac{1}{4}h^2 F_1|_{0,2j-1} + \frac{1}{2}h^2 F_1|_{1,2j-1} + \frac{1}{2}h^2 F_1|_{0,2j} + \frac{1}{2}h^2 F_1|_{1,2j} + \frac{1}{4}h^2 F_1|_{0,2j+1}.$$

For $\varphi_O \equiv \varphi_{2N,2j}$, $0 < j < N$ we get

$$(2.46) \qquad \frac{1}{6}h^2 \dot{u}_{2N,2j-2} + \frac{1}{3}h^2 \dot{u}_{2N-2,2j} + h^2 \dot{u}_{2N,2j} + \frac{1}{3}h^2 \dot{u}_{2N-2,2j+2}$$

$$+\frac{1}{6}h^2 \dot{u}_{2N,2j+2} - \frac{1}{2}D_u u_{2N,2j-2} - D_u u_{2N-2,2j} + 2D_u u_{2N,2j}$$

$$-\frac{1}{2}D_u u_{2N,2j+2} - D_u z_{2N-1,2j-1} + \frac{1}{2}D_u z_{2N,2j-1} + \frac{1}{2}D_u z_{2N-1,2j}$$

$$-\frac{1}{2}D_u z_{2N-2,2j+1} + D_u z_{2N-1,2j+1} - \frac{1}{2}D_u z_{2N-1,2j+2}$$

$$= \frac{1}{4}h^2 F_1|_{2N,2j-1} + \frac{1}{2}h^2 F_1|_{2N-1,2j} + \frac{1}{2}h^2 F_1|_{2N,2j} + \frac{1}{2}h^2 F_1|_{2N-1,2j+1}$$

$$+\frac{1}{4}h^2 F_1|_{2N,2j+1}.$$

For $\varphi_O \equiv \varphi_{0,2N}$, we have

$$(2.47) \qquad \frac{1}{6}h^2 \dot{u}_{0,2N-2} + \frac{1}{3}h^2 \dot{u}_{2,2N-2} + \frac{2}{3}h^2 \dot{u}_{0,2N} + \frac{1}{6}h^2 \dot{u}_{2,2N}$$

$$-\frac{1}{2}D_u u_{0,2N-2} + D_u u_{0,2N} - \frac{1}{2}D_u u_{2,2N} - \frac{1}{2}D_u z_{1,2N-2}$$

$$+D_u z_{1,2N-1} - \frac{1}{2}D_u z_{2,2N-1}$$

$$= \frac{1}{4}h^2 F_1|_{0,2N-1} + \frac{1}{2}h^2 F_1|_{1,2N-1} + \frac{1}{4}h^2 F_1|_{0,2N} + \frac{1}{4}h^2 F_1|_{1,2N}.$$

For $\varphi_O \equiv \varphi_{2i,2N}$, $0 < i < N$ we have

$$(2.48) \quad \frac{1}{3}h^2 \dot{u}_{2i,2N-2} + \frac{1}{3}h^2 \dot{u}_{2i+2,2N-2} + \frac{1}{6}h^2 \dot{u}_{2i-2,2N} + h^2 \dot{u}_{2i,2N}$$

$$+\frac{1}{6}h^2 \dot{u}_{2i+2,2N} - D_u u_{2i,2N-2} - 0.5 D_u u_{2i-2,2N} + 2 D_u u_{2i,2j}$$

$$-\frac{1}{2}D_u u_{2i+2,2N} - \frac{1}{2}D_u z_{2i+1,2N-2} - D_u z_{2i-1,2N-1} + \frac{1}{2}D_u z_{2i,2N-1}$$

$$+D_u z_{2i+1,2N-1} - \frac{1}{2}D_u z_{2i+2,2N-1} + \frac{1}{2}D_u z_{2i-1,2N}$$

$$= \frac{1}{2}h^2 F_1|_{2i,2N-1} + \frac{1}{2}h^2 F_1|_{2i+1,2N-1} + \frac{1}{4}h^2 F_1|_{2i-1,2N} + \frac{1}{2}h^2 F_1|_{2i,2N}$$

$$+\frac{1}{4}h^2 F_1|_{2i+1,2N}.$$

For $\varphi \equiv \varphi_{2N,2N}$, we have

$$(2.49) \quad \frac{1}{6}h^2 \dot{u}_{2N,2N-2} + \frac{1}{6}h^2 \dot{u}_{2N-2,2N} + \frac{1}{3}h^2 \dot{u}_{2N,2N} - \frac{1}{2}D_u u_{2N,2N-2}$$

$$-\frac{1}{2}D_u u_{2N-2,2N} + D_u u_{2N,2N} - D_u z_{2N-1,2N-1} + \frac{1}{2}D_u z_{2N,2N-1}$$

$$+\frac{1}{2}D_u z_{2N-1,2N} = \frac{1}{4}h^2 F_1|_{2N,2N-1} + \frac{1}{4}h^2 F_1|_{2N-1,2N} + \frac{1}{4}h^2 F_1|_{2N,2N}.$$

Eq. (2.41) - Eq. (2.49) form a sparse linear system $A\dot{u}_{2h} = b_u$ of $n_{evol} = (N+1)^2$ equations for the derivatives of the solution component u_{2h} at grid nodes x_O, $O \in \mathcal{E}_{2h}$. The matrix is stored in compressed sparse column (CSC) representation for the use with the $UMFPACK$ solver, which we use to solve the system. The system of equations $A\dot{v}_{2h} = b_v$ for the derivatives of the second solution component v_{2h} is derived analogously.

§2.2. Integration in time

By the spatial discretization of (2.14) and (2.15), two linear systems were derived for the derivatives of the solution components u_{2h}, v_{2h}

$$(2.50) \qquad\qquad\qquad A\dot{u}_{2h} = b_u,$$

$$(2.51) \qquad\qquad\qquad A\dot{v}_{2h} = b_v.$$

Being aware of other results [16, 17, 20], where the authors emphasize the necessity of using the efficient time-integration methods to allow a reliable comparison to standard

methods, we selected the modified Runge-Kutta 4th order method with the adaptive time step selection for the integration of (2.50) and (2.51) in time.

At each step of the Runge-Kutta method we first interpolate the solution u_{2h}, v_{2h} on x_P, $P \in \mathcal{E}_h$ using (2.33) - (2.35). Then we assembly and solve the linear system for the terms z_h, w_h. We continue with computation of (2.38) - (2.40) which is needed for the evaluation of terms $F_1(u_{2h} + z_h, v_{2h} + w_h)|_P$ and $F_2(u_{2h} + z_h, v_{2h} + w_h)|_P$ at nodes x_P, $P \in \mathcal{E}_h$ during the numerical integration of right-hand sides in (2.14), (2.15). Then we update the vectors b_u and b_v in (2.50) and (2.51) respectively prior to solving these systems.
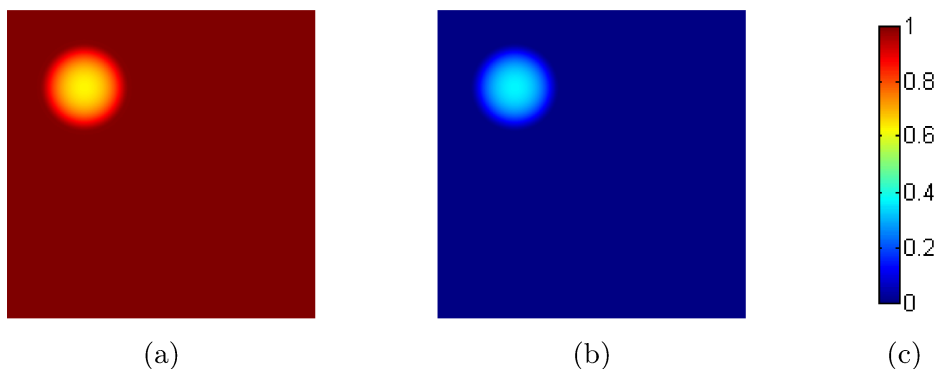

Figure 3. Example of the initial conditions for the component u and v of the Gray-Scott model are depicted in (a) and (b) respectively. Color scale used in the following figures is depicted in (c).

§3.   Numerical results

In this section we present an example of numerical results. We applied the finite element nonlinear Galerkin scheme to the numerical solution of the initial-boundary value problem for the Gray-Scott model (1.9)-(1.10) introduced in Section 1.

For the quantitative comparison we used the common finite difference scheme with the discretization the Laplace operator given by the classical five-point stencil and model parameter values $D_u = 1 \cdot 10^{-5}$, $D_v = 1 \cdot 10^{-6}$, $F = 0.025$, $k = 0.05$, $L = 0.5$ leading to nontrivial dynamics. Numerical simulations were performed on meshes with 401×401 and 801×801 grid nodes. Initial condition v_0 for the component v was a spot-like function in the upper left corner of the domain Ω defined by the exponential function

$$\exp(-1/(1 - ((x - x_0)(x - x_0) + (y - y_0)(y - y_0))/\varepsilon)$$

for $x_0 = y_0 = L/4$ and $\varepsilon = 0.00625$. The initial condition for the component u was computed as $u_0 = 1.0 - v_0$, see Fig. 3. The range of integration in time was $0 \le t \le 800$. Numerical results at times $t = 500$ and $t = 800$ are depicted in Fig. 4, Fig. 6 for the finite

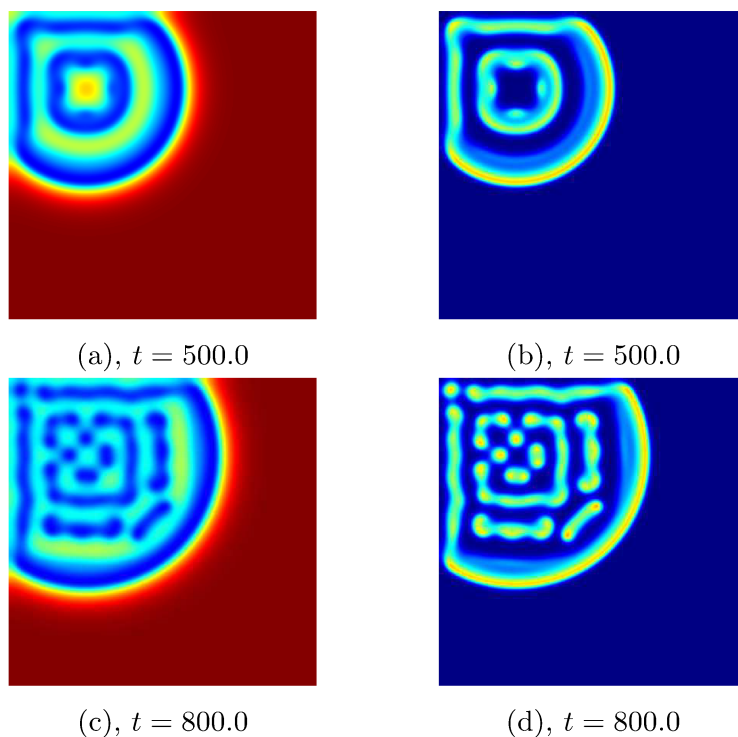(a), $t = 500.0$ (b), $t = 500.0$

(c), $t = 800.0$ (d), $t = 800.0$

Figure 4. Numerical simulation of the Gray-Scott model by the finite difference method (401 × 401 grid nodes). Both solution components u (left), v (right) are given.

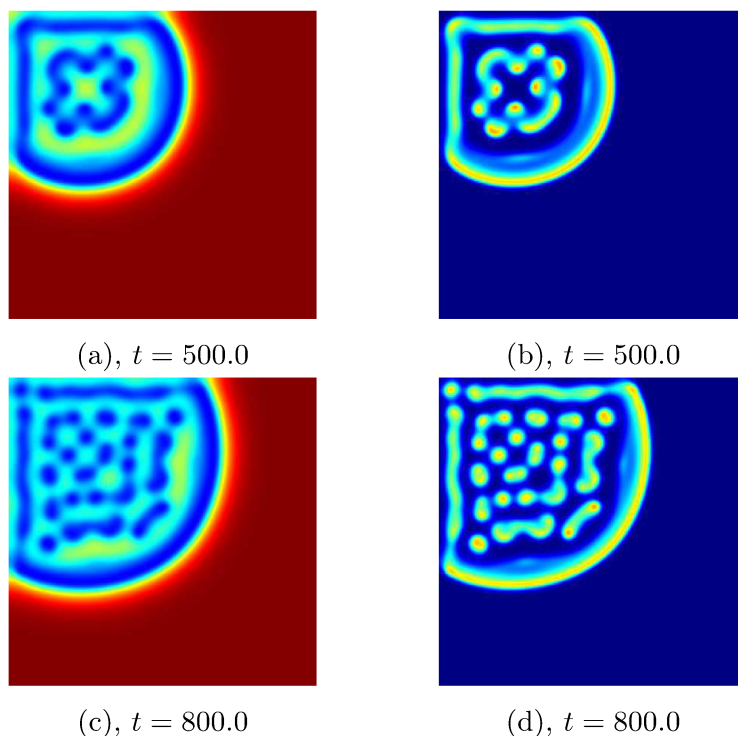(a), $t = 500.0$ (b), $t = 500.0$

(c), $t = 800.0$ (d), $t = 800.0$

Figure 5. Numerical simulation of the Gray-Scott model by the finite element nonlinear Galerkin method (401 × 401 grid nodes). Both solution components u (left), v (right) are given.

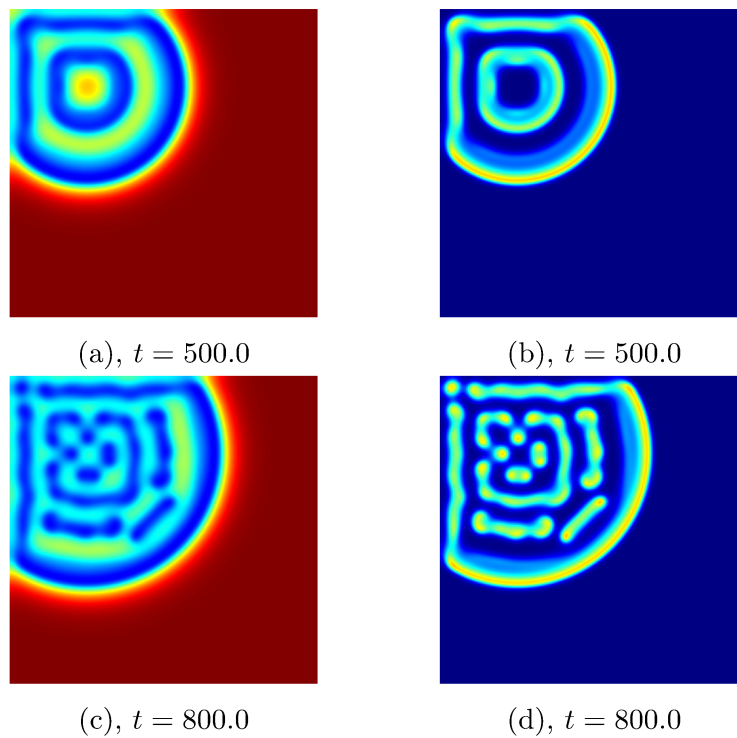(a), $t = 500.0$ · (b), $t = 500.0$

(c), $t = 800.0$ · (d), $t = 800.0$

Figure 6. Numerical simulation of the Gray-Scott model by the finite difference method (801×801 grid nodes). Both solution components u (left), v (right) are given.

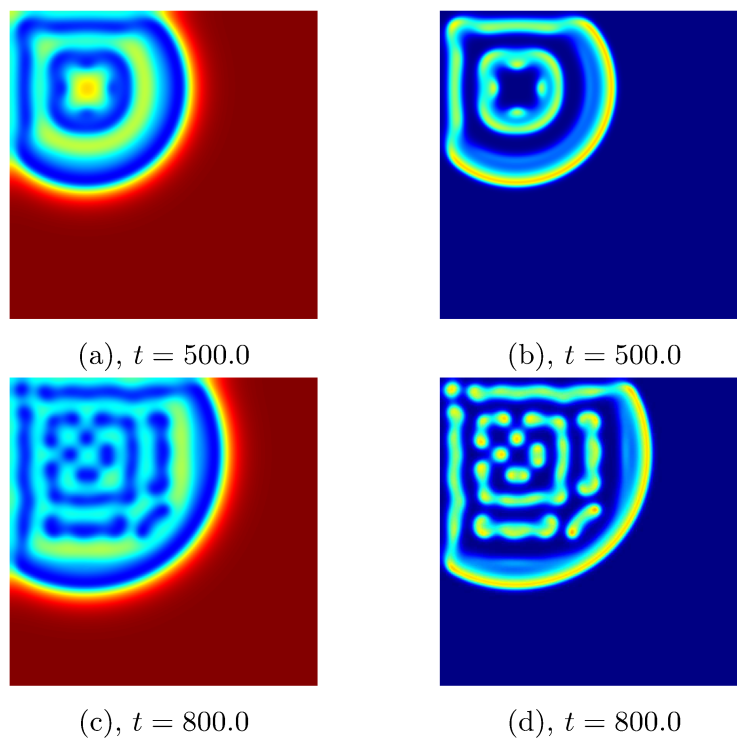(a), $t = 500.0$ · (b), $t = 500.0$

(c), $t = 800.0$ · (d), $t = 800.0$

Figure 7. Numerical simulation of the Gray-Scott model by the finite element nonlinear Galerkin method (801×801 grid nodes). Both solution components u (left), v (right) are given.
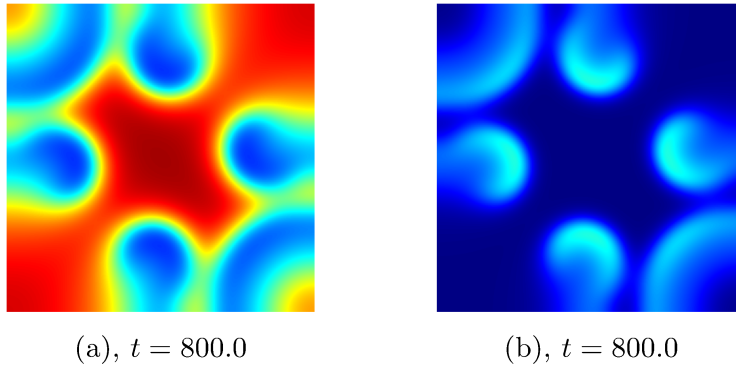
(a), $t = 800.0$ (b), $t = 800.0$

Figure 8. Other example of patterns where quantitative agreement of numerical results between finite difference and finite element nonlinear Galerkin methods applied to the solution of the Gray-Scott model was observed. Both solution components u (left), v (right) are given.

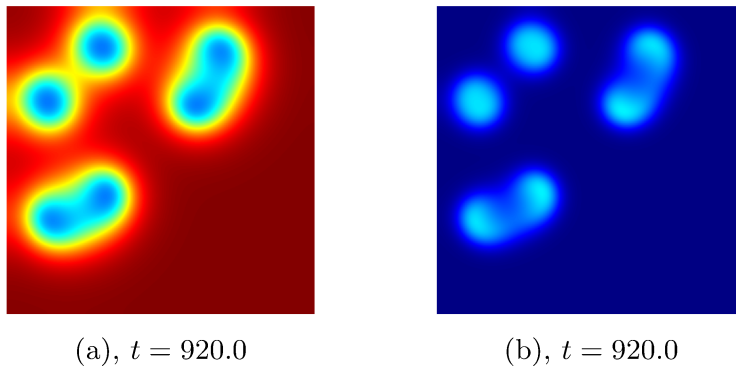(a), $t = 920.0$ (b), $t = 920.0$

Figure 9. Other example of patterns where quantitative agreement of numerical results between finite difference and finite element nonlinear Galerkin methods applied to the solution of the Gray-Scott model was observed. Both solution components u (left), v (right) are given.

difference scheme and in Fig. 5, Fig. 7 for the finite element nonlinear Galerkin method respectively. Both numerical approaches provide quantitatively the same results for the finer mesh. When using the coarser mesh, the difference in the numerical solutions is larger. Other examples of patterns where agreement of numerical results by both methods was obtained are given in Fig. 8 and Fig. 9. Model parameters $D_u = 2 \cdot 10^{-5}$, $D_v = 1 \cdot 10^{-5}$, $F = 0.02$, $k = 0.05$, $L = 0.5$ and $D_u = 2 \cdot 10^{-5}$, $D_v = 1 \cdot 10^{-5}$, $F = 0.022$, $k = 0.059$, $L = 0.5$ respectively were used.

§ 4.   Conclusion

In this paper we applied a particular finite element nonlinear Galerkin method to the numerical solution of the Gray-Scott reaction-diffusion model in two spatial dimen-

sions on a regular square numerical grid and described details of how the the numerical scheme is derived. The modified Runge-Kutta method with adaptive time step selection was used for integration in time. We provide example numerical results, which demonstrate that the nonlinear Galerkin finite element scheme (2.3)-(2.5) produce quantitatively the same results as the standard finite difference scheme. Comparison with a standard scheme was used to verify the numerical results.

References

[1] Foias, C. and Manley, O. and Temam, R., Modelling of the interaction of small and large eddies in two dimensional turbulent flows, *Mat. Mod. Numer. Anal.*, vol. 22, **1** (1988), 93–118.

[2] Marion, M. and Temam, R., Nonlinear Galerkin Methods, *SIAM J Numer. Anal.*, vol. 26, **5** (1989), 1139–1157.

[3] Marion, M., Approximate inertial manifolds for reaction-diffusion equations in high space dimension, *Journal of Dynamics and Differential Equations*, vol. 1, **3** (1989), 245–267.

[4] Temam, R., On the nonlinear Galerkin Methods, *Numerical Combustion*, Lecture Notes in Physics, Springer Berlin / Heidelberg, 1989, 461–471.

[5] Laminie, J. and Pascal, F. and Temam, R., Nonlinear Galerkin method with finite element approximation, *Twelfth International Conference on Numerical Methods in Fluid Dynamics*, Lecture Notes in Physics, Springer Berlin / Heidelberg, vol. 371, (1990), 278–282.

[6] Dubois, T. and Jauberteau, F. and Temam, R., The nonlinear Galerkin method for the two and three dimensional Navier-Stokes equations, *Twelfth International Conference on Numerical Methods in Fluid Dynamics*, Lecture Notes in Physics, Springer Berlin / Heidelberg, vol. 371, (1990), 116–120.

[7] Marion, M. and Temam, R., Nonlinear Galerkin Methods: The Finite Element Case, *Numer. Math.*, vol. 57, **1** (1990), 205–226.

[8] Pascal, F. and Basdevant, C., Nonlinear Galerkin method and subgrid-scale model for two-dimensional turbulent flows, *Theoretical and Computational Fluid Dynamics*, vol. 3, **5** 1992, 267–284.

[9] Laminie, J. and Pascal, F. and Temam, R., Implementation of finite element nonlinear Galerkin methods using hierarchical bases, *Computational Mechanics*, vol. 11, **5** 1993, 384–407.

[10] Dubois, T. and Temam, R., The nonlinear Galerkin method applied to the simulation of turbulence in a channel flow, *Thirteenth International Conference on Numerical Methods in Fluid Dynamics*, Lecture Notes in Physics, Springer Berlin / Heidelberg, vol. 414, (1993), 150–154.

[11] Dubois, T. and Jauberteau, F. and Temam, R., Solution of the incompressible Navier-Stokes equations by the nonlinear Galerkin method, Journal of Scientific Computing, vol. 8, **2** 1993, 167–194.

[12] Chen, M. and Temam, R., Nonlinear Galerkin method in the finite difference case and wavelet-like incremental unknowns, *Numerische Mathematik*, Springer Berlin / Heidelberg, vol. 64, **1** 1993, 271-294.

[13] Li, K. and He, Y. and Xiang, Y., Full discrete nonlinear Galerkin method for the Navier-Stokes equations, *Applied Mathematics - A Journal of Chinese Universities*, vol. 9, **1** 1994, 11–30.

[14] Ait Ou Amni, A. and Marion, M., Nonlinear Galerkin methods and mixed finite-elements: two-grid algorithms for the Navier-Stokes equations, *Numer. Math.*, **68** (1994), 189–213.

[15] Marion, M. and Xu, J., Error Estimates on A New Nonlinear Galerkin Method Based on Two-grid Finite Elements, *SIAM J. Numer. Anal.*, vol. 32, **4** (1995), 1170–1184.

[16] García-Archilla, B. and de Frutos, J., Time integration of the non-linear Galerkin method, *IMA Journal of Numerical Analysis*, vol. 15, **2** 1995, 221–224.

[17] García-Archilla, B., Some practical experience with the time integration of dissipative equations, *J. Comput. Phys.*, vol. 122, **1** 1995, 25–29.

[18] Debussche, A. and Dubois, T. and Temam, R., The nonlinear Galerkin method: A multiscale method applied to the simulation of homogeneous turbulent flows, *Theoretical and Computational Fluid Dynamics*, vol. 7, **4** 1995, 279–315.

[19] Dettori, L. and Gottlieb, D. and Temam, R., A nonlinear Galerkin method: The two-level Fourier-collocation case, *Journal of Scientific Computing*, vol. 10, **4** 1995, 371–389.

[20] Nabh, G. and Rannacher, R., A comparative study of nonlinear Galerkin finite element methods for dissipative evolution problems, preprint, IWR, University of Heidelberg, Germany, 1996.

[21] Bronstering, R. Simulation of reaction-diffusion systems by nonlinear Galerkin methods, *Proceedings of the 3rd workshop on Modelling of Chemical Reaction Systems*, IWR, University of Heidelberg, Germany, 1996.

[22] Šembera, J. and Beneš, M., Nonlinear Galerkin Method for Reaction-Diffusion Systems Admitting Invariant Regions, *Journal of Comp. and Appl. Math.*, vol. 136, **1-2** 2001, 163–176.

[23] He, Y. and Hou, Y. and Mei, L., Global Finite Element Nonlinear Galerkin Method for the Penalized Navier-Stokes Equations, *J. Comp. Math.*, vol. 19, **6** 2001, 607–616.

[24] Gray, P. and Scott, S. K., Autocatalytic reactions in the isothermal, continuous stirred tank reactor: oscillations and instabilities in the system $A + 2B \to 3B$, $B \to C$, *Chem. Eng. Sci.*, **39** 1984, 1087–1097.

[25] Doelman, A., Pattern formation in the one-dimensional Gray-Scott model, *Nonlinearity*, **10** 1997, 523–563.

[26] Nishiura, Y. and Ueyama, D., Self-Replication, Self-Destruction, and Spatio-Temporal Chaos in the Gray-Scott model, *Forma*, **15** 2000, 281–289.

[27] Nishiura, Y. and Ueyama, D., Spatio-temporal chaos for the Gray-Scott model, *Physica D*, vol. 150, 2001, 137–162.

[28] Dkhil, F. and Logak, E. and Nishiura, Y., Some analytical results on the Gray-Scott model, *Asymptotic Analysis*, **39** 2004, 225–261.

[29] Davis, T. A. and Duff, I. S., An unsymmetric-pattern multifrontal method for sparse LU factorization, *SIAM Journal on Matrix Analysis and Applications*, vol. 18, **1** 1997, 140–158.

[30] Davis, T. A. and Duff, I. S., A combined unifrontal/multifrontal method for unsymmetric sparse matrices, *ACM Transactions on Mathematical Software*, vol. 25, **1** 1999, 1–19.

[31] Davis, T. A., A column pre-ordering strategy for the unsymmetric-pattern multifrontal method, *ACM Transactions on Mathematical Software*, vol. 30, **2** 2004, 165–195.

[32] Davis, T. A., Algorithm 832: UMFPACK, an unsymmetric-pattern multifrontal method, *ACM Transactions on Mathematical Software*, vol. 30, **2** 2004, 196–199.

[33] Mach, J. and Beneš, M., Nonlinear Galerkin FEM method applied to the system of reaction-diffusion equations in one spatial dimension, in preparation.